RSC Advances

ROYAL SOCIETY OF CHEMISTRY

www.rsc.org/advances

Table of contents:

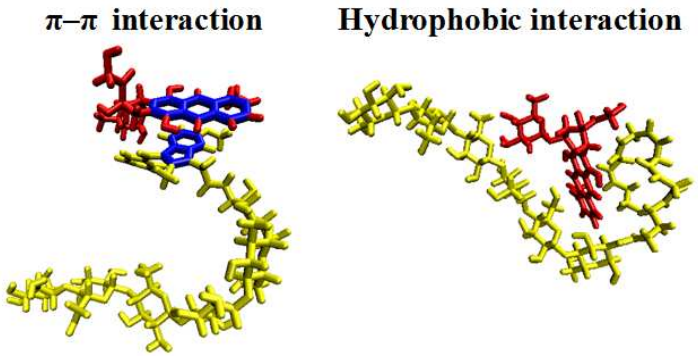

Both π–π interaction and hydrophobic interaction were found essential to Doxorubicin loading on hydrophobically modified chitosan oligosaccharides.

Molecular dynamics study on the interaction between doxorubicin and hydrophobically modified chitosan oligosaccharide†

Peng Shan,[a,b,‡] Jia-Wei Shen,[a,‡] Dong-Hang Xu,[c] Li-Yun Shi,[a] Jie Gao,[d] Ya-Wei Lan,[d] Qi Wang,[d,*] and Xiao-Hong Wei [a,*,§]

[a] *School of Medicine, Hangzhou Normal University, Hangzhou 310036, PR China*

[b] *College of Material, Chemistry and Chemical Engineering, Hangzhou Normal University, Hangzhou 310036, PR China*

[c] *Second Affiliated Hospital, College of Medicine, Zhejiang University, Hangzhou 310009, PR China*

[d] *Soft Matter Research Center and Department of Chemistry, Zhejiang University, Hangzhou 310027, PR China*

[‡] *Peng Shan and Jia-Wei Shen contributed equally to this work.*

* *Corresponding author. E-mail addresses: qiwang@zju.edu.cn, xiaohongwei1@foxmail.com.*

[§] *Corresponding author. Fax: +86-571-28869344.*

† *Electronic supplementary information (ESI) available.*

Abstract

Doxorubicin (DOX) is a broad spectrum anti-tumor anthracycline antibiotic used in cancer chemotherapy, but it has certain limitation on therapeutic effect due to non-specific targeting. Amphiphilic polymeric micelle drug delivery systems could help to improve the activity and selectivity of DOX against tumor cells. In this study, molecular dynamics simulation was performed to investigate the interaction between DOX and ten hydrophobic-acid modified chitosan oligosaccharides (COS). The π–π interaction in the systems with aromaticity has been found contributing a great part of the van der Waals interaction and playing a significant role in the DOX loading process. The encapsulated DOX by long-chain fatty acid grafted COS mainly depends on the high binding strength and sandwiched configuration where the hydrophobic interaction is essential to the encapsulation process. The solvent structure around DOX and grafted COS was found to have relationship with the way DOX and drug carrier binding to each other. Moreover, the results derived by our computational model were compared to the experimental data obtained in our lab and the data available in the literatures. It was found that the interaction strength between DOX and hydrophobically modified COS has strong correlation to the experimental quantities like encapsulation efficiency and drug loading rate.

Keywords: Drug delivery; Chitosan oligosaccharide; Hydrophobic modification; Doxorubicin; Drug encapsulation; Molecular dynamics

1 Introduction

Doxorubicin (DOX), as shown in Fig. 1(a), is a broad spectrum anti-tumor anthracycline antibiotic used in cancer chemotherapy. It belongs to the class of cycle-phase nonspecific drugs which can kill tumor cells with variety of cell cycles.[1] It can inhibit both cellular DNA and RNA synthesis and has effects on a variety of tumors.[2] However, as DOX doesn't have the capability of identifying tumor cells from normal cells, it has great toxicity to normal cells while killing tumor cells.[3] That's the reason why it is not the first choice of anticancer drugs. Amphiphilic polymeric micelles could form core-shell structures in the aqueous solution by self-assembling. The hydrophobic blocks constitute the hydrophobic core and the hydrophilic blocks constitute the hydrophilic shell.[4] Hydrophobic drugs can be encapsulated into the hydrophobic core through

physical or chemical interaction.[5] The study of Hu *et al*. have shown that the compatibility between the hydrophobic drugs and the hydrophobic blocks is the main factor that affect the drug loading ability.[6] Better compatibility between the hydrophobic drugs and the hydrophobic blocks lead to larger amount of drug loading and slower drug release rate. In recently years, plenty of amphiphilic polymeric micelle drug delivery systems have been designed and developed to improve the activity and selectivity of DOX against tumor cells, to extend the circulation time *in vivo* and to reduce its side effects, thus improve the therapeutic effect.[7-11]

Chitin is a long-chain polymer of N-acetylglucosamine (a derivative of glucose) via covalent β-1,4 linkages. It could be found in many places and the total biomass of chitin in the natural world is second only to cellulose. Chitosan is a linear polysaccharide which could be obtained by deacetylation of chitin. The structure of chitosan is very similar to cellulose. In the C2 position of glucose residues in chitosan there is an amino group instead of hydroxyl group in the same position in cellulose. However, the hydroxyl group is neutral, while the amino group is alkaline. Compared to its parent chitin, the solubility of chitosan in water is improved, but it is still very limited. Chitosan oligosaccharide (COS), the oligomer of chitosan, is the degradation product of chitosan, and it is the only alkaline oligosaccharide so far. The solubility of COS is greatly improved compared to chitosan. Its good biocompatibility and biodegradability provide it as a good candidate for drug delivery in biomedical field. Many studies have shown that COS has the effects of anti-tumor, anti-mutagenic and anti-oxidation. In addition, COS can lower blood sugar and blood pressure, regulate blood lipids and protect the liver. Moreover, it also has the effects of improving immunity, anti-bacterial, anti-viral *etc.*[12] Because of these excellent properties of COS, its hydrophobically modified amphiphilic polymeric micelle and application to drug delivery and gene delivery have received more and more attention in recent years .[11,13-16]

Molecular dynamics (MD) simulation is a powerful tool which computes the motions of individual molecules and obtains detailed information on the interesting systems and phenomena. During the simulation, the equation of motion of the whole system is numerically and iteratively integrated, and the positions and momentum of every molecule or atom are reserved. Therefore, MD simulation helps us better understand the atomic-level structure and dynamics information which are difficult to be observed in the experiments.[17] In recent years, MD simulation is widely

used in drug delivery system to study the properties and interaction of molecules.[18] It is especially good at handling issues which are difficult to be investigated in laboratory experiments for drug delivery.[19] In this study, MD simulation was used to investigate the interaction between the drug DOX and ten different hydrophobically modified COS as well as the mechanism of drug loading in the COS system. Besides, how factors such as functional groups, hydrophobic property of the hydrophobically modified COS influence the drug loading process was analyzed, and the contributions of the van der Waals and electrostatic interaction to the drug loading process were discussed. Moreover, the results derived by the computational model were compared to the experimental data obtained in our lab and the data available in the literatures. At the end of this paper, the common features of the ideal grafts were summarized, and this may help to understand and design the ideal molecules for efficient and controlled DOX delivery systems.

2 Computational methods

In order to understand the mechanism of the interaction between DOX and hydrophobically modified COS, ten different acids (as shown in Table 1) were selected to modify the hydrophobicity of COS. These acids include Indomethacin (IMN) and Salicylic Acid (SAL), which have aromatic rings; Alpha-Linolenic Acid (LNL), Arachidonic Acid (ACD), Docosa-4,7,10,13,16,19-Hexaenoic Acid (HXA), Linoleic Acid (EIC), Icosapent (EPA) and Stearic Acid (STE), which are long-chain fatty acids and have high hydrophobicity; Cholic Acid (CHD) and Lipoic Acid (LPA), both of which have cyclic ring structure but don't have aromaticity. The molecular structures of them were shown in Fig. 1. In all MD simulations in this study, the initial structures of these acids were taken from the Protein Data Bank (PDB), and their ligand IDs are shown in Table 1. The initial structure of COS hexamer was taken from Glycam Biomolecule Builder (designed for carbohydrates and related molecules). The energy minimization of COS hexamer was performed using the GLYCAM06 parameters.[20] After that, the carboxyl groups of ten acids were conjugated to the amino groups of the COS hexamer. Then the structures of all hydrophobically modified molecules were geometrically optimized by Gaussian 03 package,[21] using the HF/6-31G basis set.[22] The atomic charges of modified COS hexamer were also calculated by using HF/6-31G method. All MD simulations were executed by Gromacs 4.5.2.[23] The force field parameters of all organic molecules (including DOX) were taken from the general

amber force field (GAFF) of the Antechamber package, which contains parameters of most organic and drug molecules constituted by C, H, O, N, S, P and halogen.[24]

The grafted COS chain and a DOX molecule were putted into a cube box with box size of 5.0 nm. The center of mass of the complex was placed into the center of the box. Then, 3200 TIP3P[25] water molecules were added into each box. Therefore, there were ten systems in our MD simulations (the system label was shown in Table 1). These systems were energy minimized with both the steepest descent and conjugate gradient algorithm (the maximum number of steps and the energy step size of two kind of energy minimization were set to 50000 and 0.01 nm). Afterwards, 200 ps of NVT equilibrium and 300 ps of NPT equilibrium were conducted sequentially. After all these pretreatments, MD simulation was carried out in NPT ensemble. The time step was set to 1 fs in all MD simulations. Temperature and pressure were controlled to 300 K and 1 bar by V-rescale[26] and Parrinello-Rahman[27] methods, respectively. Periodic boundary conditions were used in all dimensions and the long-range electrostatic interactions were treated by Particle Mesh Ewald (PME).[28] The intercept of PME and the cutoff of non-bonded interaction were both 1.0 nm. The method of LINCS[29] was used to constrain all the bonds. The total simulation time was 50 ns and the last 30 ns trajectory was used to analyze the data. The total interaction energy between drug and carriers in all systems in MD simulations is defined by equation (1):

$$E_{\text{int}} = E_{\text{complex}} - E_{\text{drug}} - E_{\text{carrier}} \quad (1)$$

Where E_{int} stands for the total (non-bonded) interaction energy between the drug and the carrier, E_{complex}, E_{drug} and E_{carrier} are the potential energies of the drug-carrier complex, drug, and carrier, respectively. Previous studies have shown that the interaction energy could qualitatively estimate the binding strength of complex systems.[30,31]

3 Results and discussion

3.1 π–π interaction

The configurations and relative positions of the drug and carriers in the simulation trajectory were carefully checked. One distinguish phenomenon is the relative close distance and parallel orientation between the aromatic rings in both DOX and IMM, as well as in DOX and SAL. Fig. 2(a) and 2(b) show the snapshot of the COS/IMN and COS/SAL system in the last frame of the

MD simulation. In the trajectory of both COS/IMN and COS/SAL systems, the aromatic rings in DOX and carrier were always adopt the configuration that parallel to each other. The distances between the parallel aromatic rings during these two simulations were around 0.34 nm, and this is the typical distance between two conjugated system with π–π interaction formed.[33] Therefore, it strongly indicated that the π–π interaction was formed in these two systems. To estimate the binding strength of the drug to carrier, Fig. 2(c) and 2(d) also shown the interaction energy between the drug and carrier in two systems that changed with the simulation time. The fluctuation of interaction energy of these two systems is relatively small in the last 30 ns. This indicates that both of these two system achieved metastable state. The averaged total interaction energy of COS/IMN and COS/SAL system in the last 30 ns are –100.06 and –139.34 kJ/mol, as shown in Table 2. It is difficult to directly estimate the contribution of the π–π interaction to the total interaction energy, however, they were accounted into the vdW interaction in the force field. The vdW interaction energies in these two systems are –93.95 and –59.85 kJ/mol. This difference probably due to the fact that in IMN there are two aromatic ring involving a five-membered heterocycle while in SAL there are only one phenyl ring. Therefore, IMN could form much stronger π–π interaction with DOX than SAL. The contribution of the vdW interaction to the total interaction between the drug DOX and IMN is around 94%, which also indicate the important role of π–π interaction. Fig. 3 shows the normalized density of DOX around drug carrier's surface, which indicates the location of the drug around carrier as well as the binding strength of drug to the carriers. From Fig. 3(a) it was found that the peaks of DOX density distribution around drug carrier in both COS/IMN and COS/SAL systems are much larger and sharper than that in COS/CHD and COS/LPA systems. This proves that DOX in both COS/IMN and COS/SAL systems are much closer to the hydrophobically modified COS chains, and the affinity of the drug to IMN and SAL is higher than other two systems. Both of the peaks locate around 0.34 nm away from the carrier's surface, which mainly attribute to the close π–π interaction distance. From the above analysis, it could be inferred that the π–π interaction in the system of COS/IMN and COS/SAL plays a significant role in the drug loading process.

3.2 Single chain encapsulation

During the simulations, the phenomenon of long-chain fatty acid grafted COS chain encapsulating

DOX was observed. For example, at the initial time of the simulations, DOX and the hydrophobically modified COS chain was separated in COS/EIC, COS/EPA and COS/STE systems, as shown in Fig. 4 (snapshot at 0 ns). Then, DOX move closer to the hydrophobic group of long-chain fatty acid (Fig. 4, snapshot at 20 ns) accompanied by the bending of the flexible long-chain fatty acid chain. Eventually, DOX was sandwiched between the end of long-chain fatty acid and the COS at the end of the simulation (Fig. 4, snapshot at 50 ns). As the DOX is highly hydrophobic, the sandwiched configuration buried the hydrophobic part of the drug-carrier complexes and maximized the hydrophobic interaction between the drug and carriers. From Fig. 3(b) it could be found that the height and width of the normalized density of DOX around the carrier's surface in these three systems were very close. Compared to COS/IMN system, the heights of the density peak in these three systems were lower while the heights of the density peak in COS/SAL system were larger than that in COS/EPA and COS/STE system. However, the widths of the density peak in these three long-chain fatty acid grafted COS systems were larger, indicating that the hydrophobic interaction in COS/EPA and COS/STE systems were not site-specific while the π–π interaction in COS/IMN and COS/SAL systems were highly depend on the interaction site and restricted conformations. Fig. 4(c) to 4(d) shows the total interaction energies between the drug and carrier in COS/EIC, COS/EPA and COS/STE systems with respect to the simulation time. Since the long chain fatty acids of these three were extremely flexible, the fluctuation of the interaction energy was high during the simulations. However, the averaged total interaction energy (over last 30 ns trajectory) between the drug and carrier in these three systems were –144.10 kJ/mol, –149.50 kJ/mol and –164.09 kJ/mol, respectively. They were the highest three in all systems, as shown in Table 2. The main reason of high fluctuation of the energy may due to the fact that DOX was sandwiched between both of the hydrophobic and hydrophilic end and it interacted with both of two ends. The electrostatic interaction energies in these systems were relatively smoother than the vdW interaction, and the total interaction generally follow the trend of fluctuation of the vdW interaction. This confirm the high flexibility of EIC, EPA and STE modified COS and indicate that the hydrophobic interaction contribute a large part to the total interaction. Previous theoretical method had well study the kinetics of random copolymers,[34] but in MD simulation the fluctuation of the chain conformation may led to non-sufficient sampling of the system. However, the high density of the drug DOX around carrier as well as the strong

interaction energy could still qualitatively estimate the binding affinity of DOX to EIC, EPA and STE modified COS. The encapsulated DOX by single chain mainly depend on the high binding strength and sandwiched configuration where the hydrophobic interaction probably plays an important role.

3.3 More systems

In this study, totally six long-chain fatty acid systems were selected to hydrophobically modified the COS chain. Among them, three systems (COS/EIC, COS/EPA and COS/STE) have been observed the phenomenon of single chain encapsulation while other three long-chain fatty acid modified COS systems did not exhibit this phenomenon. However, these long-chain fatty acids are very flexible and the encapsulation of the drug is a dynamic process which may occur beyond the simulation time. It is difficult to judge if other three fatty acids (LNL, ACD and HXA) modified COS could encapsulate the drug DOX on the basis of limited simulation time. In Fig. 5(a) to 5(c), the interaction energy between drug and carrier in these three systems with respect to the simulation time were plotted. It could be found that the averaged total interaction energy between drug and carrier of these systems are much smaller than that in COS/EIC, COS/EPA and COS/STE systems. The main reason is that they did not form the sandwiched configuration of the complex, thus the hydrophobic interactions were much weaker than that in COS/EIC, COS/EPA and COS/STE systems.

In addition to the six long-chain fatty acids and two acids which have aromatic rings, COS/CHD and COS/LPA systems were also checked. The change of the interaction energy between the drug and carrier of these two systems were shown in Fig. 5(d) and 5(e). The fluctuations of the interaction energy were large for these two systems, which indicates the poor stability of drug-carrier complexes. From Fig. 3(a) it could be found that the density distribution of DOX in these two systems are smallest in the near region around the carriers in all ten systems, which implies the poor binding affinity of DOX to CHD and LPA modified COS.

3.4 Solvent effect

Since the COS chain was hydrophobically modified by ten different acid, the water structure around the carrier may change and has certain influence on the DOX binding process. We have

checked the radial distribution function (RDF) of oxygen (in modified COS chain)-oxygen (in water) and oxygen (in DOX)-oxygen (in water) for all ten systems. In general, the system with long-chain fatty acid grafted COS encapsulating DOX has the lowest RDF around both drug carrier and DOX (e.g. COS/STE system), as shown in Fig. S1 and Fig. S2. This is because the strong hydrophobic interaction between DOX and hydrophobic long-chain could drive a great number of water molecules out of the DOX-carrier interface. The hydrophobic interaction in fatty acid grafted COS systems were not site-specific while the π–π interaction in COS/IMN and COS/SAL systems were highly depend on the interaction site, therefore, the number of water molecules drove out by π–π interaction is less than that drove out by hydrophobic interaction, and the RDFs in COS/IMN and COS/SAL systems are higher than that in systems having single chain encapsulation. In COS/CHD and COS/LPA systems, due to the loose binding of DOX to drug carrier, the RDFs in both systems are highest. We summarized RDFs in three typical systems (COS/IMN, COS/STE and COS/CHD) discussed above and plotted them in Fig. 6. It indicates the correlation between solvent structure and the way DOX and drug carrier bind to each other (as well as the interaction energy).

3.5 Hydrogen bond analysis

As hydrogen bond between drug and carrier has been found having great influence on the drug loading rate[18], the inter-molecular hydrogen bonds formed between DOX and hydrophobically modified COS in all systems have been checked and listed in Table 2. In addition, the intra-molecular (DOX-DOX, carrier-carrier) hydrogen bonds were also shown Table 2. The criterion of hydrogen bonding for the donor-acceptor cutoff distance is 0.35 nm, and the cutoff angle of hydrogen-donor-acceptor is 30° (including 0°). Here the OH and NH groups are donors, and receptors could be O and N. From the analysis of simulation trajectory, it was found that if DOX was away from the hydrophilic COS end and close to the hydrophobic end, the electrostatic interactions were generally small (*e.g.*, COS/ACD, COS/IMN, *etc.*). If DOX located close to the hydrophilic COS end which increase the possibility of forming inter-molecular hydrogen bonds, the electrostatic interactions increased significantly (*e.g.*, COS/EPA and COS/STE). Moreover, the electrostatic interaction between the drug and carrier has very strong correlation to the number of inter-molecular hydrogen bonds. Fig. 7 show the linear fit of electrostatic interaction and number

of hydrogen bonds between DOX and carrier. A linear equation was obtained: $y = -38.86x - 9.09$ ($R^2 = 0.9265$). In the AMBER force field there is no special term that consider for hydrogen bond. The hydrogen-bond energy still arises from the dipole-dipole interaction of the donor and acceptor groups and added to the electrostatic potential. This is the reason why electrostatic interaction energy increase with the increasing of number of hydrogen bonds. In general, the strength of hydrogen bond formed by OH and NH (acceptor) with O and N (receptor) range from 5 to 30 kJ/mol. The fitted equation implies that the effect of increasing a hydrogen bond to the electrostatic interaction between DOX and carrier is around 39 kJ/mol. This is not surprising since the forming of hydrogen bond decrease the distance between DOX and carrier, and both of DOX and carrier could adjust their conformation to make the polar group complementary to each other. Therefore, the increasing of electrostatic interaction energy between DOX and carrier is not only attributes to the energy of forming hydrogen bonds but also due to the increasing of electrostatic interaction between other polar groups with closer distance between DOX and carrier. One has to notice that this empirical equation based on the statistic of ten hydrophobically modified COS and has certain limitation to apply to other systems. However, one could use it to estimate the strength of electrostatic interaction between DOX and hydrophobically modified COS on the basis of number of hydrogen bonds formed. Moreover, this equation could be more accurate base on more testing of other hydrophobically modified COS systems.

Due to the relative rigid conformation of DOX, hydroxyl group and carbonyl oxygen in conjugated aromatic ring in DOX forms two stable intra-molecular hydrogen bonds (O-H…O) in all systems. However, the number of carrier-carrier intra-molecular hydrogen bond is various due to the flexibility of hydrophobically modified COS and the way that DOX-carrier binds to each other (discussed in section 3.1, 3.2 and 3.3).

3.6 Comparison to the experimental data

To verify our computational model, the simulation results were compared to the experimental data obtained in our lab (for details, see Electronic supplementary information) and the data available in the literatures. Table 3 lists the micelle size, encapsulation efficiency (*EE*) and drug loading (*DL*) rate in the experiments as well as the interaction energy in our calculations for COS/IMN, COS/EIC and COS/CHD systems. The experimental data for cholic acid modified COS and DOX

system is not available in the literatures, so we chose the available experimental data of deoxycholic acid (DXC) modified COS and DOX system instead. Here the encapsulation efficiency and drug loading rate are defined as equation (2) and (3):

$$EE\% = (W_e / W_t) \times 100\% \quad (2)$$

$$DL\% = [W_e / (W_e + W_c)] \times 100\% \quad (3)$$

Where W_e is the amount of drug encapsulated in the micelle, W_t is the total amount of drug added initially, and W_c is the amount of drug carrier. Although in our simulations only one molecule of DOX and one single chain of hydrophobically modified COS were considered, the drug loading rate in the experiments in these systems listed in Table 3 qualitatively follow the trend of the interaction strength between DOX and carriers. For example, the COS/EIC system has the strongest interaction in the computational model and this system has largest drug loading rate of 15.17% in the experiments. The encapsulation efficiency of these systems follows a similar way, but COS/IMN system has a little higher value than COS/EIC system. This may due to the fact that the COS/IMN system in the experiments has bigger micelle size (shown in Table 3) and more volume to encapsulate drug molecules. One has to notice that in the experiments many properties like structure, chain length and concentration *etc.* of drug carrier could affect the encapsulation efficiency and drug loading rate. Therefore, it is difficult to directly compare the interaction strength between drug and carrier in simulation and the quantity (encapsulation efficiency, drug loading rate *etc.*) in the experiments, but they have strong correlations as discussed above. In this study, we focused on the simple model of one chain of hydrophobically modified COS and drug, and this model gives reasonable estimation of the interaction strength (between drug and carriers) which has strong correlation with some quantities in the experiments. Recently, great progress have been achieved in the field of nanoparticle interacting with biological system.[36] Better understanding of the structure, self-assembling and thermodynamics of the targeting nanoparticles could greatly improve the design of drug delivery system. Our future work will focus on the structure, thermodynamic and dynamic properties of the nanoparticle systems consist of drug DOX and longer chain of hydrophobically modified COS in a series of concentrations.

4 Conclusion

In this study, MD simulation was used to investigate the interaction between the drug DOX and ten hydrophobically modified COS as well as the mechanism of DOX loading in the hydrophobically modified COS system. How aromaticity and hydrophobic property of the hydrophobically modified COS influence the interaction strength between DOX and carrier as well as the DOX loading process were analyzed and discussed. The π–π interaction in the system with aromaticity (COS/IMN and COS/SAL) contributes a big part of the van der Waals interaction and plays a significant role in the DOX loading process. The encapsulated DOX by long-chain fatty acid grafted COS chain mainly depend on the high binding strength and sandwiched configuration where the hydrophobic interaction plays an important role. The solvent structure around DOX and grafted COS was found to have relationship with the way DOX and drug carrier bind to each other. It was also found that the electrostatic interaction between the drug and carrier has linear relationship to the number of hydrogen bonds. Moreover, the results derived by our computational model were compared to the available experimental data. It was found that the interaction strength between DOX and hydrophobically modified COS has strong correlation to the experimental quantities (encapsulation efficiency and drug loading rate). From our computational model, two types of ideal hydrophobic block were suggested to hydrophobically modified COS for DOX delivery in experimental evaluation. The first one is the long-chain fatty acids like STE and EPA. Similar to hydrophobic polymers, the experimental conditions of getting long-chain fatty acid grafted COS is simple and easy to achieve. The second one is acid with aromaticity like SAL (often seen in non-steroidal anti-inflammatory drugs, such as Montelukast, Bexarotene, Bezafibrate, Carprofen, *etc.*). Molecules which have both strong hydrophobicity and aromaticity may form more stable core-shell structure with DOX and have high drug loading rate. In conclusion, this work may help to understand and design the ideal molecules for efficient and controlled DOX delivery systems. Our future work will pay more efforts on the structure and thermodynamic properties of the systems consist of drug DOX and longer chain of hydrophobically modified COS in a series of concentration. The dynamics of the self-assembling of hydrophobically modified COS and the effect of the micelle size to the DOX encapsulation efficiency and loading rate will be studied.

Acknowledgments

The authors acknowledge the financial supports of National Natural Science Foundation of China (Nos. 30973683, 21273200 and J1210042), Zhejiang Provincial Natural Science Foundation (Y14H300015 and Y14B030033).

References

1 W. H. Mondesire, W. Jian, H. X. Zhang, J. Ensor, M. C. Hung, G. B. Mills and F. Meric-Bernstam, *Clin. Cancer Res.*, 2004, **10**, 7031-7042.

2 R. L. Momparler, M. Karon, S. E. Siegel and F. Avila, *Cancer Res.*, 1976, **36**, 2891-2895.

3 S. W. Wang, E. A. Konorev, S. Kotamraju, J. Joseph, S. Kalivendi and B. Kalyanaraman, *J. Biol. Chem.*, 2004, **279**, 25535-25543.

4 M. L. Adams, A. Lavasanifar and G. S. Kwon, *J. Pharm. Sci.*, 2003, **92**, 1343-1355.

5 A. Harada, H. Togawa and K. Kataoka, *Eur. J. Pharm. Sci.*, 2001, **13**, 35-42.

6 Y. Hu, X. Q. Jiang, Y. Ding, L. Y. Zhang, C. Z. Yang, J. F. Zhang, J. N. Chen and Y. H. Yang, *Biomaterials*, 2003, **24**, 2395-2404.

7 K. Y. Lee, J. H. Kim, L. C. Kwon and S. Y. Jeong, *Colloid Polym. Sci.*, 2000, **278**, 1216-1219.

8 J. H. Park, S. Kwon, M. Lee, H. Chung, J. H. Kim, Y. S. Kim, R. W. Park, I. S. Kim, S. B. Seo, I. C. Kwon and S. Y. Jeong, *Biomaterials*, 2006, **27**, 119-126.

9 J. Zhang, X. G. Chen, Y. Y. Li and C. S. Liu, *Nanomed. Nanotechnol. Biol. Med.*, 2007, **3**, 258-265.

10 G. Kwon, M. Naito, M. Yokoyama, T. Okano, Y. Sakurai and K. Kataoka, *J. Control. Release*, 1997, **48**, 195-201.

11 Y. Z. Du, L. Wang, H. Yuan, X. H. Wei and F. Q. Hu, *Colloids Surf. B: Biointerfaces*, 2009, **69**, 257-263.

12 V. Dodane and V. D. Vilivalam, *Pharm. Sci. Technol. Today*, 1998, **1**, 246-253.

13 F. Q. Hu, X. L. Wu, Y. Z. Du, J. You and H. Yuan, *Eur. J. Pharm. Biopharm.*, 2008, **69**, 117-125.

14 F. Q. Hu, M. D. Zhao, H. Yuan, J. You, Y. Z. Du and S. Zeng, *Int. J. Pharm.*, 2006, **315**, 158-166.

15 S. Y. Chae, S. Son, M. Lee, M. K. Jang and J. W. Nah, *J. Control. Release*, 2005, **109**, 330-344.

16 S. Son, S. Y. Chae, C. Choi, M. Y. Kim, V. G. Ngugen, J. K. Kweon, M. K. Jang and J. W. Nah, *Macromol. Res.*, 2004, **12**, 573-580.

17 E. R. Lindahl, *Methods Mol. Biol.*, 2008, **443**, 3-23.

18 M. Subashini, P. V. Devarajan, G. S. Sonavane and M. Doble, *J. Mol. Model.*, 2011, **17**,

1141-1147.

19 Y. Y. Li and T. J. Hou, *Curr. Med. Chem.*, 2010, **17**, 4482-4491.

20 K. N. Kirschner, A. B. Yongye, S. M. Tschampel, J. Gonzalez-Outeirino, C. R. Daniels, B. L. Foley and R. J. Woods, *J. Comput. Chem.*, 2008, **29**, 622-655.

21 M. J. Frisch, G. W. Trucks, H. B. Schlegel, G. E. Scuseria, M. A. Robb, J. R. Cheeseman, *et al*. Gaussian03, Revision E.01, Gaussian, Inc., Pittsburgh PA, 2007.

22 A. Almond, A. Brass and J. K. Sheehan, *J. Phys. Chem. B*, 2000, **104**, 5634-5640.

23 D. van der Spoel, E. Lindahl, B. Hess, G. Groenhof, A. E. Mark and H. J. C. Berendsen, *J. Comput. Chem.*, 2005, **26**, 1701-1718.

24 J. M. Wang, R. M. Wolf, J. W. Caldwell, P. A. Kollman and D. A. Case, *J. Comput. Chem.*, 2004, **25**, 1157-1174.

25 W. L. Jorgensen, J. Chandrasekhar, J. D. Madura, R. W. Impey and M. L. Klein, *J. Chem. Phys.*, 1983, **79**, 926–935.

26 G. Bussi, D. Donadio and M. J. Parrinello. *Chem. Phys.*, 2007, **126**, 14101-14107.

27 M. Parrinello and A. Rahman, *J. Appl. Phys.*, 1981, **52**, 7182-7190.

28 T. Darden, D. York and L. Pedersen, *J. Chem. Phys.*, 1993, **98**, 10089-10092.

29 J. Zhang, J. Z. Lou, S. Ilias, P. Krishnamachari and J. Yan, *Polymer*, 2008, **49**, 2381-2386.

30 J. W. Shen, T. Wu, Q. Wang, H. H. Pan, *Biomaterials*, 2008, **29**, 513-532.

31 J. W. Shen, T. Wu, Q. Wang, Y. Kang and X. Chen, *ChemPhysChem*, 2009, **10**, 1260-1269.

32 W. Humphrey, A. Dalke and K. Schulten, *J. Mol. Graph.*, 1996, **14**, 33-38.

33 C. Janiak, *J. Chem. Soc. Dalton Trans.*, 2000, 3885-3896.

34 E. G. Timoshenko, Y. A. Kuznetsov and K. A. Dawson, Phys. Rev. E 1996, 54, 4071-4086.

35 Y. Z. Du, L. Wang, H. Yuan, X. H. Wei and F. Q. Hu, *Colloids Surf. B: Biointerfaces*, 2009, **69**, 257-263.

36 M. P. Monopoli, C. Åberg, A. Salvati and K. A. Dawson, *Nat. Nanotech*. 2012, **7**, 779-786.

Table 1 The name, ligand ID and system label of ten acids.

Name	Ligand ID	System
Indomethacin	IMN	COS/IMN
Salicylic Acid	SAL	COS/SAL
Alpha-Linolenic Acid	LNL	COS/LNL
Arachidonic Acid	ACD	COS/ACD
Docosa-4,7,10,13,16,19-Hexaenoic Acid	HXA	COS/HXA
Linoleic Acid	EIC	COS/EIC
Icosapent	EPA	COS/EPA
Stearic Acid	STE	COS/STE
Cholic Acid	CHD	COS/CHD
Lipoic Acid	LPA	COS/LPA

Table 2 The number of hydrogen bond, electrostatic interaction (Ele), vdW interaction (vdW) and total interaction energies (IE) in all systems. Data were taken from the last 30 ns trajectory of total 50 ns in MD simulations.

System	No. of H-bonds (drug-carrier)	No. of H-bonds (drug-drug)	No. of H-bonds (carrier-carrier)	Ele (kJ/mol)	vdW (kJ/mol)	IE (kJ/mol)
COS/IMN	0.00	2.00	5.03	–6.11	–93.95	–100.06
COS/SAL	1.82	2.00	5.80	–79.49	–59.85	–139.34
COS/LNL	1.03	2.00	4.56	–56.23	–60.84	–117.07
COS/ACD	0.11	2.00	5.27	–8.32	–59.73	–68.05
COS/HXA	0.28	2.00	4.55	–17.86	–50.31	–68.17
COS/EIC	0.46	2.00	4.38	–44.07	–100.03	–144.10
COS/EPA	1.79	2.00	4.51	–85.75	–63.75	–149.50
COS/STE	1.68	2.00	5.60	–74.45	–89.64	–164.09
COS/CHD	0.66	2.00	4.55	–29.16	–23.85	–53.01
COS/LPA	0.40	2.00	5.36	–27.79	–70.80	–98.59

Table 3 The micelle size, encapsulation efficiency, drug loading rate in the experiments as well as the interaction energy in our simulations for COS/IMN, COS/EIC and COS/CHD (DXC) systems

System	Micelle size(nm)	*EE* (%)	*DL* (%)	*IE* (kJ/mol)
COS/EIC[35]	205.7±2.8	75.21±2.26	15.17±0.14	–144.10
COS/IMN[a]	345.1±0.2	81.58±0.86	7.76±0.4	–100.06
COS/CHD (DXC)[7]	270.5±24.5	27.5	4.6	–53.01

[a]For more details of the synthesis and characterization of COS/IMN system, please see Electronic Supplementary Information.

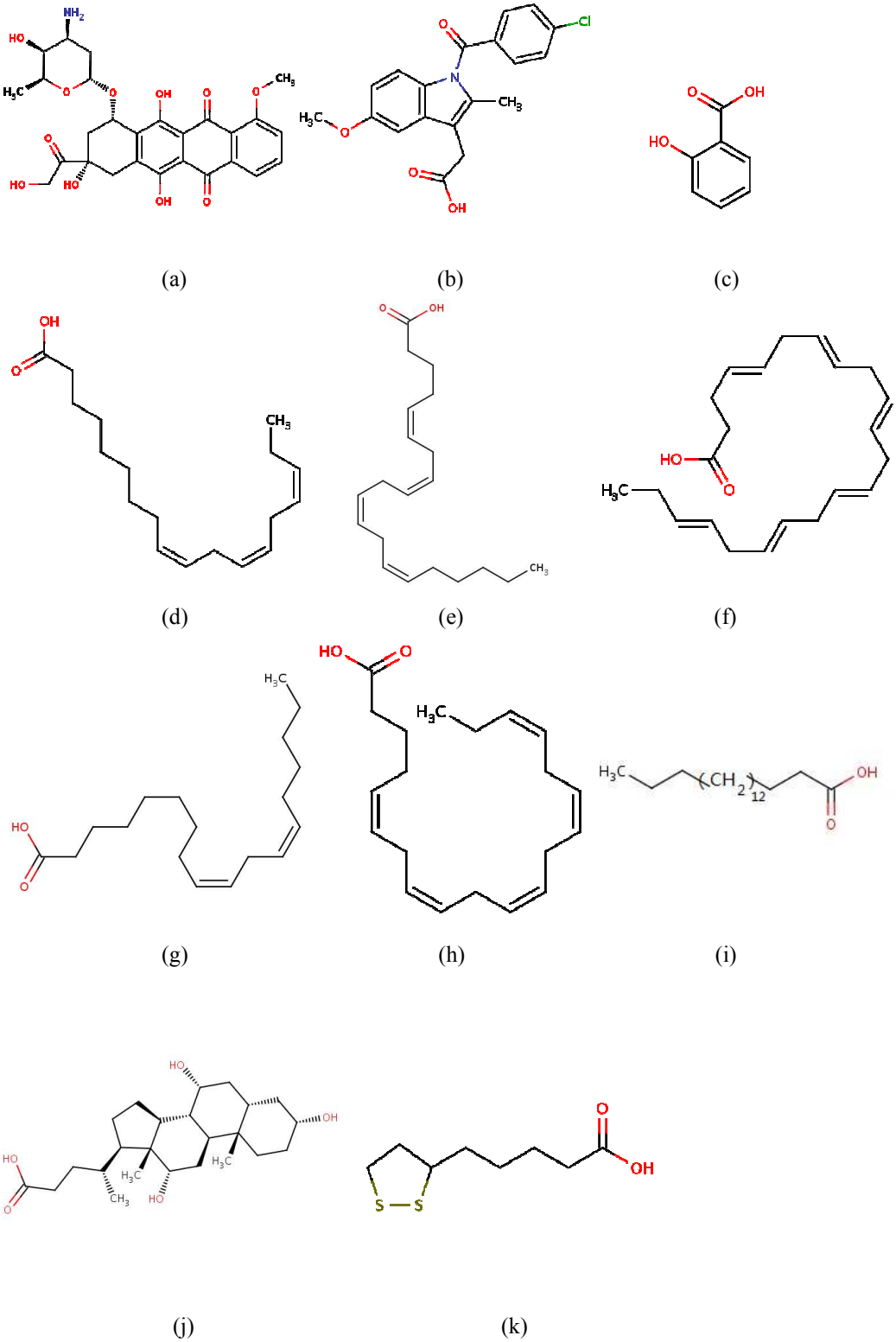

Fig. 1 Molecular structure of: (a) DOX; (b) IMN; (c) SAL; (d) LNL; (e) ACD; (f) HXA; (g) EIC; (h) EPA; (i) STE; (j) CHD; (k) LPA.

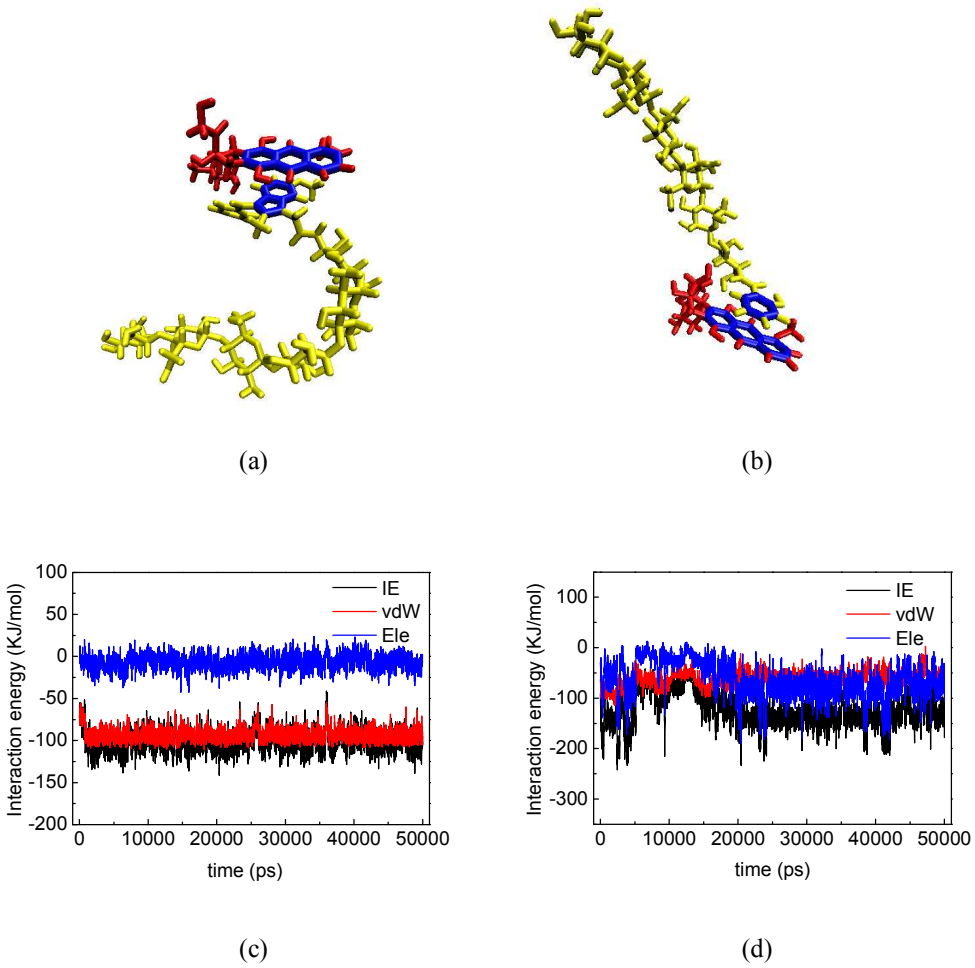

Fig. 2 (a) Snapshots of IMN grafted COS chain (yellow) and DOX (red), and (b) Snapshots of SAL grfated COS chain (yellow) and DOX (red) after 50 ns MD simulation. The aromatic rings in both drug and carrier which formed π-π stacking were colored in blue, and the water molecules were omitted for clarity; (c) The total interaction energy (IE), van der Waals interaction energy and electrostatic interaction energy between the drug and carrier in (c) COS/IMN and (d) COS/SAL systems. Visualization was carried out by VMD 1.9 package.[32]

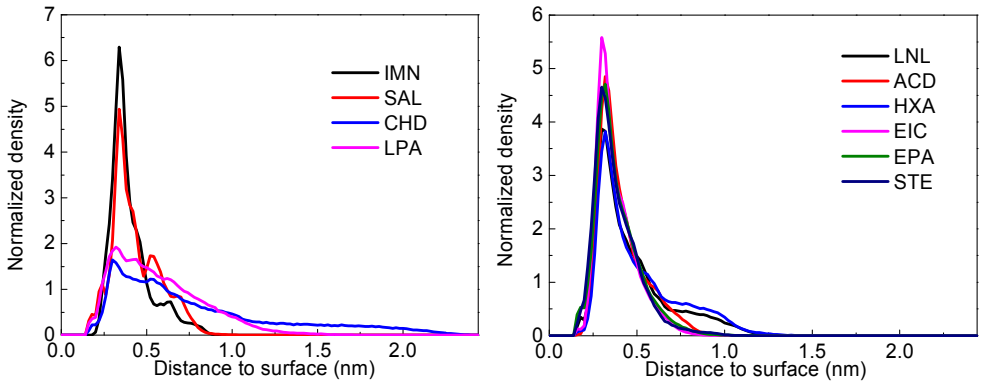

(a) (b)

Fig. 3 Normalized density of drug DOX around carrier's surface: (a) COS/IMN (black), COS/SAL (red), COS/CHD (blue) and COS/LPA (pink); (b) COS/LNL (black), COS/ACD (red), COS/HXA (blue), COS/EIC (pink), COS/EPA (green) and COS/STE (dark blue).

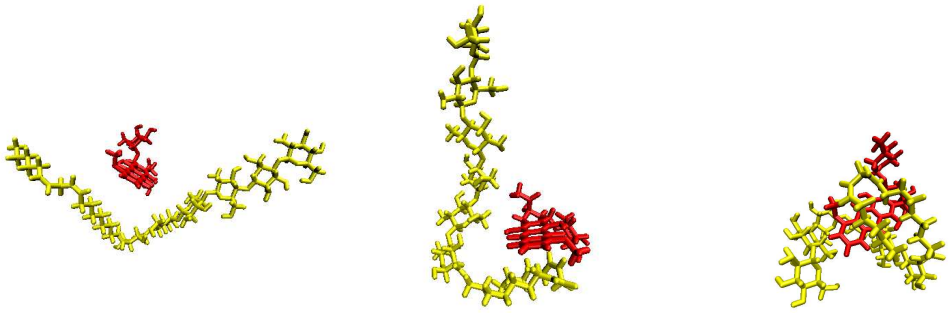

0 ns 20 ns 50 ns

(a)

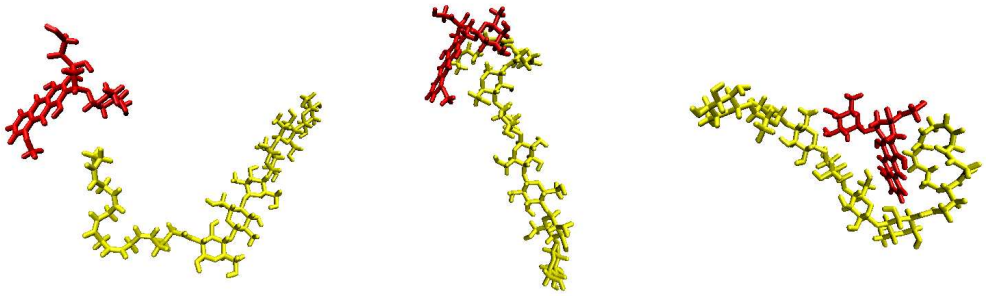

0 ns 20 ns 50 ns

(b)

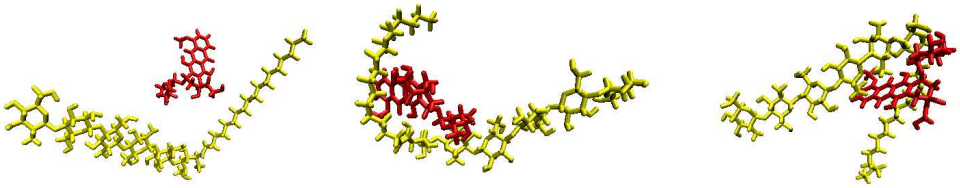

0 ns 20 ns 50 ns

(c)

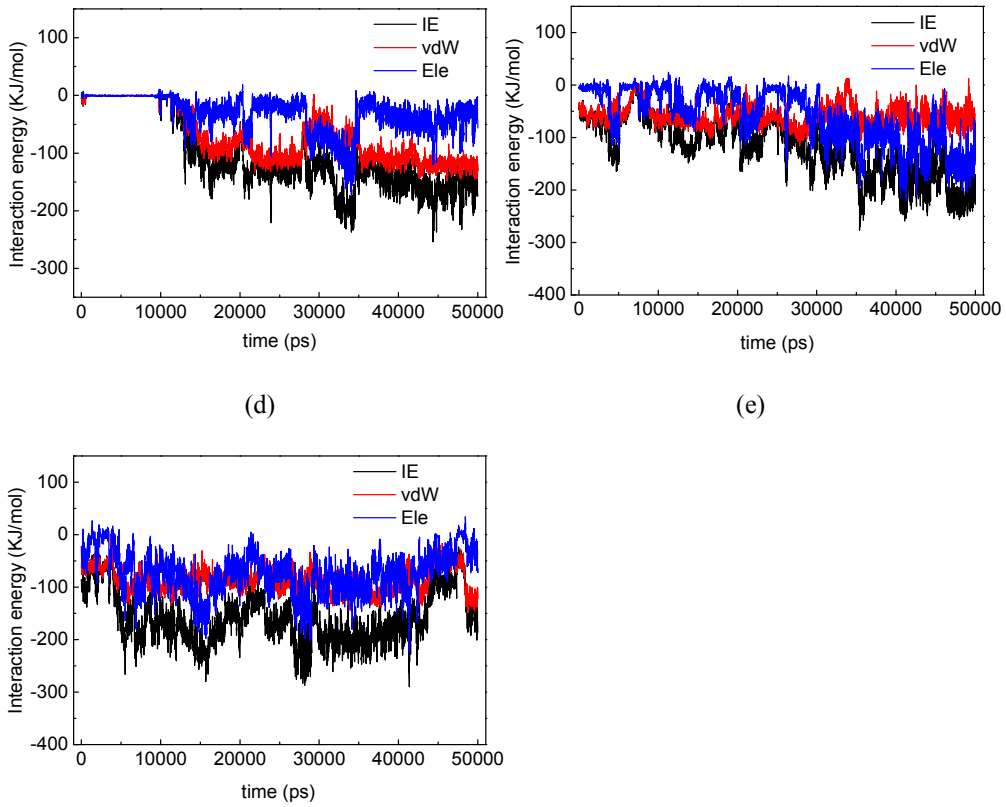

Fig. 4 (a) Snapshots of EIC grafted COS chain (yellow) and DOX (red) at 0 ns, 20 ns and 50 ns in simulations; (b) snapshots of EPA grafted COS chain (yellow) and DOX (red) at 0 ns, 20 ns and 50 ns in simulations; (c) snapshots of STE grafted COS chain (yellow) and DOX (red) at 0 ns, 20 ns and 50 ns in simulations; The total interaction energy, van der Waals interaction energy, electrostatic interaction energy between the drug and carrier in (d) COS/EIC, (e) COS/EPA and (f) COS/STE systems.

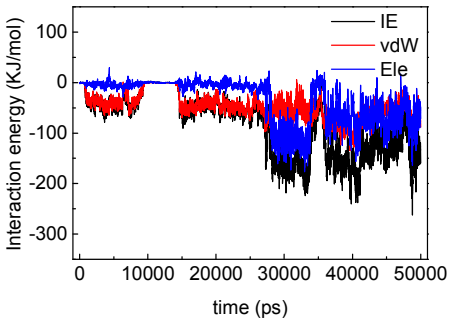

(a)

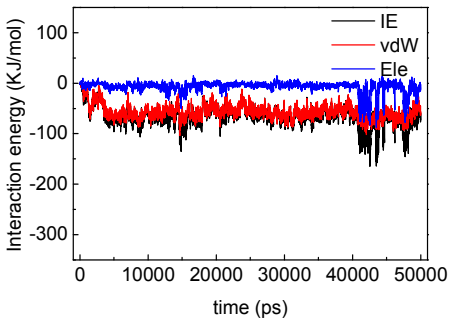

(b)

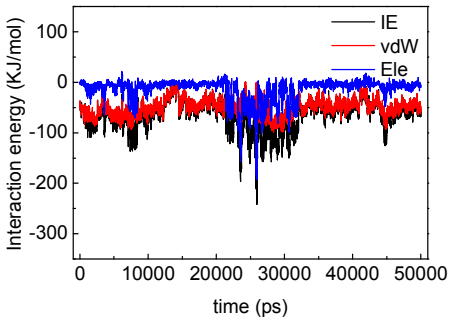

(c)

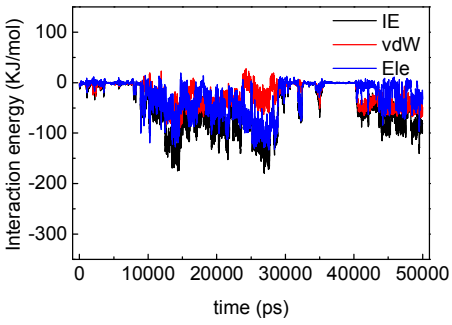

(d)

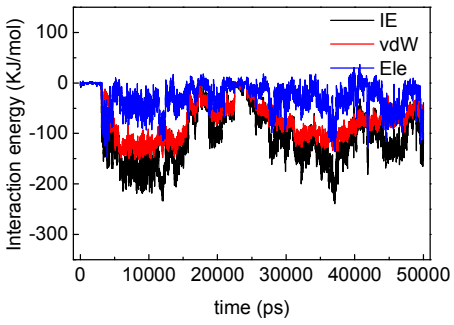

(e)

Fig. 5 Total interaction energy, van der Waals interaction energy and electrostatic interaction energy between the drug and carrier in (a) COS/LNL, (b) COS/ACD, (c) COS/HXA, (d) COS/CHD and (e) COS/LPA systems.

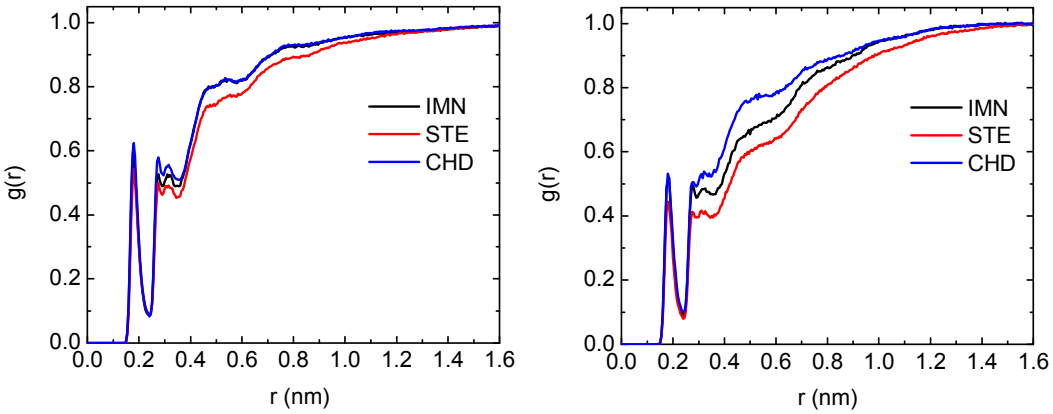

Fig. 6 (a) Radial distribution functions of oxygen (in COS/IMN chain)-oxygen (in water) (black), oxygen (in COS/STE chain)-oxygen (in water) (red) and oxygen (in COS/CHD chain)-oxygen (in water) (blue); (b) Radial distribution functions of oxygen (in DOX)-oxygen (in water) in the system of COS/IMN (black), COS/STE (red) and COS/CHD (blue).

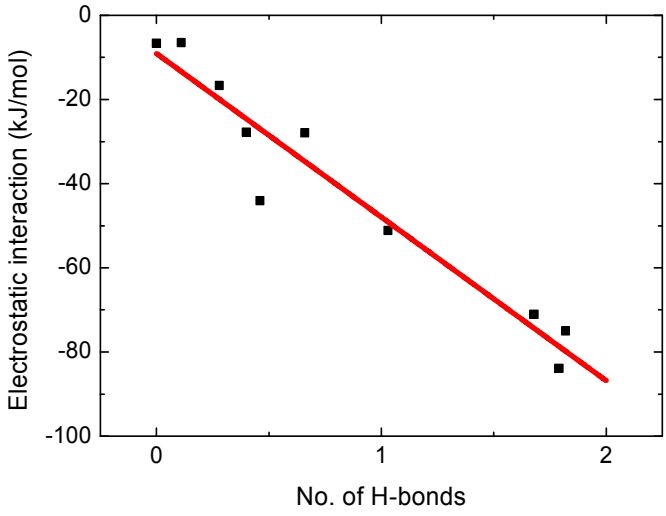

Fig. 7 Linear relationship between the electrostatic interaction energy and number of hydrogen bonds between DOX and carrier with $y = -38.86x - 9.09$ and $R^2 = 0.9265$.